

# Classical and quantum dynamics of chirped pulse dissociation of diatomic molecules

Jian-Min Yuan

*Department of Physics and Atmospheric Science, Drexel University, Philadelphia, Pennsylvania 19104*

Wing-Ki Liu

*Department of Physics, Guelph-Waterloo Program for Graduate Work in Physics (GWP), University of Waterloo, Ontario, Canada N2L 3G1*

(Received 26 June 1997)

The dissociation of a diatomic molecule by a chirped infrared laser pulse is modeled by a Morse oscillator interacting with a classical electric field with a time-dependent frequency. Our previous classical analysis in terms of bucket dynamics, in which systems within the single-node separatrices (buckets) in phase space are trapped and undergo convection to highly excited states, is found to be applicable to the more general cases of nonlinear chirping and using a realistic dipole moment function for the molecule. This route of excitation leads to a much lower dissociation threshold laser intensity when compared to the chaotic diffusion route for monochromatic excitation. Time-dependent quantum mechanical calculations of the dissociation probability based on the split-operator method are performed. It is found that the classical and quantum results agree well, and the classical resonances appear also in the quantum probabilities. Hence the classical method can be used to investigate various characteristics of the chirped pulse excitation and dissociation processes. [S1050-2947(98)03403-9]

PACS number(s): 33.80.Wz, 33.80.Gj, 03.20.+i,

## I. INTRODUCTION

The possibility of dissociating molecules by multiphoton absorption processes using infrared (IR) lasers was discovered in the early 1970s [1], and a particularly exciting aspect of this process is its isotopic selectivity [2]. The study of excitation and dissociation of molecules by IR lasers has continued to be a subject of interest [3], but experimental results are available only for polyatomic molecules. The generally accepted mechanism involves near-resonant excitations of the pumped modes which are coupled to other modes, with the other degrees of freedom serving as a bath [4]. Focusing on the excitation and dissociation aspect of a single pumped mode, one often studies the simplified problem of a diatomic molecule modeled by a Morse oscillator and driven by an IR laser [5,6]. It should be noted that the local mode concept employing the Morse oscillator has also been used extensively in the study of overtone vibrational spectra of polyatomic molecules [7].

The driven Morse oscillator [6] has been one of the paradigms in the study of classical-quantum correspondence of nonlinear (microscopic) systems [6,8,9] as well. The roles played by nonlinear resonances [10] in the dissociation dynamics of a Morse oscillator driven by a continuous or an impulsive field have been studied in detail [11,12]. As the laser intensity increases, these resonance islands begin to overlap and annihilate each other. The associated bifurcations divide the phase space into fragments filled with smaller resonance islands, periodic orbits, and other invariant phase space structures, such as homoclinic or heteroclinic aperiodic orbits [6,11]. As a result, the dynamics becomes very irregular or chaotic. We have shown that these phase space structures are often organized by the symmetry lines of the problem [12], and that the associated dissociation dynamics becomes extremely sensitive to external control param-

eters, such as the field intensity and frequency [6]. The corresponding quantum calculation [6] shows similar sensitivity, but its resolution is limited by the effective Planck constant, which is inversely proportional to the number of bound states of the Morse oscillator. Furthermore, under suitable conditions, the addition of a second laser lowers the dissociation threshold intensity considerably [13], which can be predicted using the Chirikov overlap criterion [14]. We also show that in the presence of a laser field, collisions between two atoms interacting via a Morse potential exhibit fractal scattering patterns [6].

Ideally, predictions based on nonlinear resonances should be compared with experiments directly. However, it has been shown that, at the laser intensity required for significant multiphoton IR dissociation of diatomic molecules, the ionization process actually dominates [15–17]. Thus, no experimental result on monochromatic multiphoton dissociation of neutral diatomic molecules without ionization (except the  $\text{HCl}^+$  ion [18]) has been reported to date. On the other hand, recent quantum calculations [15–17,19] showed that by using chirped laser pulses, the threshold field intensity for dissociation can be reduced to a range below that for ionization, which is achievable in present-day laboratories. A chirped laser pulse is a pulse whose frequency sweeps adiabatically with time. For molecular dissociation, it is optimal to sweep the frequency downward, since the resonant frequency decreases with energy due to anharmonicity. Furthermore, chirped pulses have been shown theoretically to be effective in selective inversion of vibrational overtones [20].

Frequency chirping also occurs in plasma physics, and particle motion in a wave with time-dependent frequency has been analyzed in terms of bucket dynamics [21,22]. Recently, we employed similar ideas to provide a physical picture for the classical dynamics of chirped pulse dissociation of a Morse oscillator [23]. For the case of a linearly chirped

pulse and a molecule with a linear dipole moment, we have shown that the system is well described by a time-dependent approximate resonant Hamiltonian in a moving frame. The system can become trapped in buckets in phase space, and carried upwards to highly excited regions by convection. This route of excitation is very different from the chaotic diffusion mechanism in fixed-frequency excitation, and requires a much lower threshold intensity for dissociation.

In this paper, we wish to study extensively the applicability of ‘‘bucket dynamics’’ to the cases of (i) nonlinear chirping and (ii) the use of a realistic dipole moment function for the molecule NO [24]. We have also carried out quantum mechanical wave packet calculations to compare with our classical dynamics results. The organization of this paper is as follows: in Sec. II, we summarize the classical analysis of the chirped pulse excitation of a Morse oscillator within the Chirikov resonant approximation, which gives rise to the concept of ‘‘bucket dynamics.’’ We will demonstrate by numerical calculation that this concept applies to the general case of nonlinear chirping and to the molecule NO with a realistic dipole moment. In Sec. III, we describe the method used in our quantum calculation, and we compare our quantum and classical results in Sec. IV. The paper is concluded with a discussion in Sec. V.

## II. BUCKET DYNAMICS

We first study the classical dynamics of chirped pulse dissociation. The diatomic molecule is represented by a Morse oscillator, with the Hamiltonian in dimensionless units given by [11,15,23]

$$H_0(x,p) = \frac{1}{2}p^2 + \frac{1}{2}(e^{-2x} - 2e^{-x}). \quad (1)$$

Here energy is measured in terms of  $2D$ , with  $D$  being the dissociation energy of the diatomic molecule, and length is measured from the equilibrium bond length in terms of the range of the Morse oscillator  $1/\alpha$ . In terms of the action-angle variables  $(i, \theta)$ , the Morse Hamiltonian takes the simple form  $H_0(i) = -\frac{1}{2}(1-i)^2$ . The Cartesian and action-angle variables are related by [11,13,25]

$$x = \ln \left[ \frac{1 - \sqrt{1 - (1-i)^2 \cos \theta}}{(1-i)^2} \right], \quad (2)$$

$$p = \frac{\omega \sqrt{1 - \omega^2 \sin \theta}}{1 - \sqrt{1 - \omega^2 \cos \theta}},$$

where  $\omega = \omega(i) = \partial H_0 / \partial i = 1 - i$  is the frequency of unperturbed motion. This shows that as the energy of the molecule increases with the action  $i$ , the unperturbed frequency decreases. When  $i = 1$ ,  $H_0(i) = 0$  and the molecule dissociates.

The molecule is coupled to the chirped laser pulse by the electric dipole interaction. Thus the total time-dependent Hamiltonian is

$$H(x,p,t) = H_0(x,p) - B\mu(x)\cos[\Omega(t)t]. \quad (3)$$

In Eq. (3),  $\mu(x)$  is the reduced dipole moment function of the molecule normalized to  $d\mu(0)/dx = 1$  at the equilibrium

bond distance. The angular frequency is measured in terms of the harmonic frequency of the Morse oscillator,  $\omega_0 = \alpha\sqrt{2D/M}$ , where  $M$  is the reduced mass of the molecule. The driving amplitude  $B$  is related to the electric field  $E$  of the laser by  $B = q_e E / (2\alpha D)$  with  $q_e$  the effective charge of the molecule and a square pulse is assumed for the calculations reported below. The driving frequency is assumed to be of the form

$$\Omega(t) = \Omega_0 \left[ 1 - \frac{1}{2} \left( \frac{t}{\tau_{sw}} \right)^{n_p} \right]. \quad (4)$$

Both the linear chirping case with  $n_p = 1$  and the nonlinear chirping case with  $n_p = 2$  will be studied in detail. We assume that  $\Omega(t)$  is a slowly varying function of time, so that adiabatic invariance allows us to define instantaneous resonance frequencies and actions of the Hamiltonian of Eq. (3) satisfying

$$\Omega(t) = m\omega(i_m) \quad \text{or} \quad i_m(t) = 1 - \Omega(t)/m, \quad (5)$$

where  $m = 1, 2, \dots$

We have shown in Ref. [23] that for the case of a linear dipole moment function  $\mu(x) = x$ , molecules near the  $m$ th resonance zone with action close to  $i_m(t)$  can be described in a ‘‘moving frame’’ by the resonant Hamiltonian

$$K(\psi, J) = \frac{J^2}{2} + V(\psi), \quad (6)$$

$$V(\psi) = -BG_m \cos m\psi - \frac{\phi}{m} \frac{d}{dt}(\dot{\Omega}t),$$

where

$$\psi = \frac{\Omega}{m}t - \theta, \quad J = i - i_m + \frac{\dot{\Omega}}{m}t, \quad (7)$$

and  $G_m$  is the coefficient of  $\cos m\theta$  in the Fourier expansion of  $x(\theta, i)$  of Eq. (2) evaluated at the stable fixed point of the system. The detailed derivation of Eq. (6) will be given in the Appendix. For linear chirping with  $n_p = 1$ ,  $\dot{\Omega} = -\Omega_0 / (2\tau_{sw})$  is a constant, and the resonant Hamiltonian of Eq. (6) becomes time-independent when the time dependence of the slowly varying  $i_m(t)$  is ignored. We show in Fig. 1 the potential  $V(\psi)$  and the phase space trajectories for  $K(\psi, J)$  with parameters satisfying the existence condition

$$|\dot{\Omega}| / (m^2 BG_m) < 1, \quad (8)$$

so that  $V(\psi)$  can have local maxima and minima. The fixed points of  $K$  are given by  $J = 0$  and  $\psi'_c = [2l\pi + \delta]/m$ , where  $\delta = \sin^{-1}\{[\dot{\Omega}/(m^2 BG_m)]\}$ ,  $l = 0, \pm 1, \pm 2, \dots$ ; while the saddle points are given by  $J = 0$ ,  $\psi'_s = [(2l+1)\pi + \delta]/m$ . Thus, single-node separatrices are formed which produce trapped regions called ‘‘buckets.’’ Transforming back from the moving frame to the original frame, we observe that trajectories inside the buckets will oscillate about the centers whose actions increase in time according to  $J = 0$  or

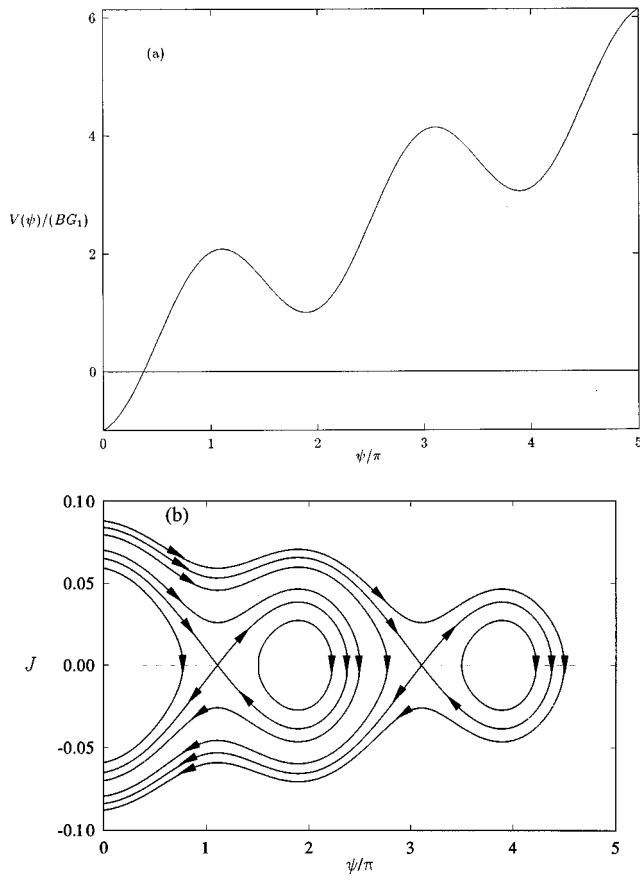


FIG. 1. (a) The potential  $V(\phi)$  and (b) phase space portrait in the moving frame for  $B=0.003$ ,  $m=1$ ,  $\Omega_0=0.9$ , and  $\tau_{sw}=2000$ .

$$i_B(t) = i_m(t) - \dot{\Omega}t/m, \quad (9)$$

and dissociate when  $i_B \sim 1$ . Trajectories in the untrapped region will not dissociate; as shown in Ref. [21], when they are far from the separatrix, the averaged action is given by  $d/dt \langle J \rangle = \dot{\Omega}/m$  or  $d/dt \langle i \rangle = 0$ , so that  $\langle i \rangle = \text{const}$ . As they approach the separatrix, they slide over to the other side of the resonance zone and move away, eventually attaining a lower value of  $\langle i \rangle$ . Such behavior has indeed been observed from trajectories generated by the exact Hamiltonian of Eq. (3) [23]. Furthermore, from their associated Poincaré maps in the moving frame, we have demonstrated in Ref. [23] that the approximate Hamiltonian of Eq. (6) does provide an accurate description of the system for the case of linear chirping  $n_p = 1$  and a linear dipole moment function  $\mu(x) = x$ . We hence arrived at the following physical picture: dissociation occurs when the system is trapped by the bucket in phase space, and transported convectively upwards in action at a rate proportional to the chirping rate.

We now wish to show that the concept of bucket dynamics applies also to the cases of nonlinear chirping, and using a realistic dipole moment function  $\mu(x)$ . We study first the case of nonlinear chirping  $n_p = 2$  with a linear dipole function  $\mu(x) = x$ . In Figs. 2(a) and 2(b), we plot the dissociating trajectories and their Poincaré maps by numerically integrating Hamilton's equations for  $\Omega_0 = 0.9$ . As before [23], the Poincaré maps of the dissociating trajectories are obtained by

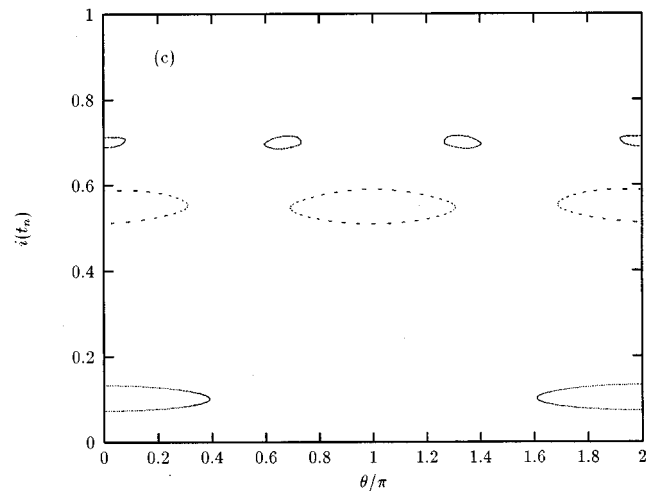
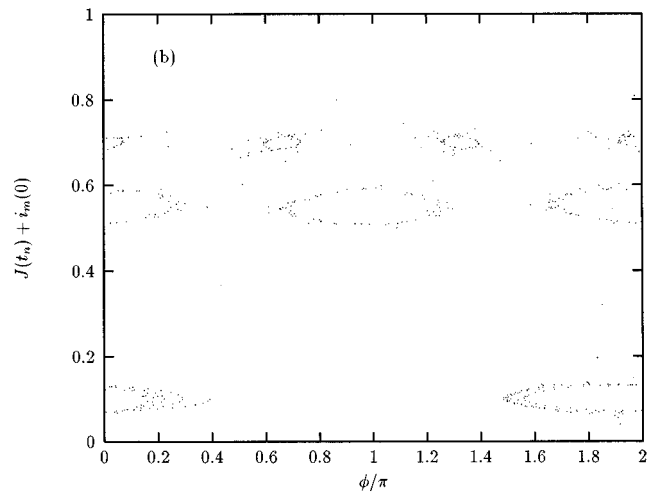
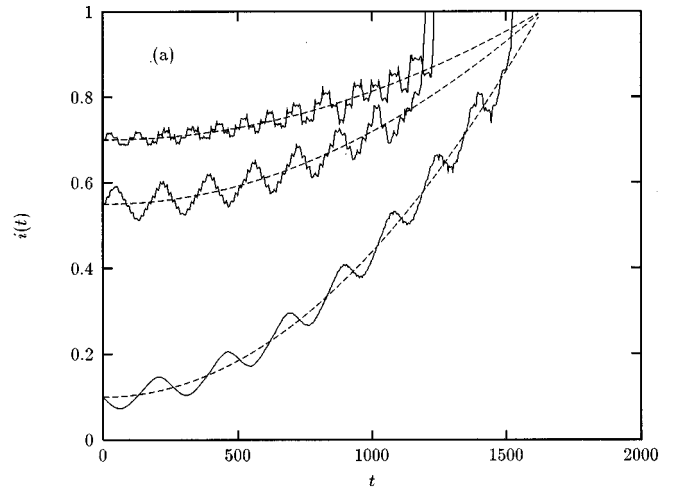


FIG. 2. Excitation using a linear dipole moment function. (a) Exact trajectories for a chirped laser pulse with parameters set at  $B=0.003$ ,  $\tau_{sw}=2000$ ,  $\Omega_0=0.9$ , and  $n_p=2$ . The initial conditions of the trajectories are  $(i(0), \theta(0)) = (0.10, 1.61\pi)$ ,  $(i(0), \theta(0)) = (0.55, 0.31\pi)$ ,  $(i(0), \theta(0)) = (0.70, 0.7333\pi)$ . The dashed lines denote the trajectories of the centers of the buckets  $i_B(t)$  given by Eq. (9) for  $m=1, 2$ , and  $3$ . (b) Poincaré surfaces of section for a chirped laser pulse with parameters and initial conditions given in (a); (c) the Poincaré surfaces of section for a fixed-frequency pulse, with parameters and initial conditions given in (a) except that  $n_p=0$ .

recording the values of the action-angle variables at times  $t_n$  satisfying  $\Omega(t_n)t_n = 2n\pi$ ,  $n=0,1,2,\dots$ , until the system dissociates. Note that at  $t_n$ ,  $\text{mod}(\theta, 2\pi) = 2\pi \text{mod}(\psi, 2\pi)$ . In Fig. 2(a), the trajectories oscillate about their corresponding centers given by Eq. (9), and the phase portraits of Fig. 2(b) again correspond to those for  $K(\psi, J)$ , and resemble the Poincaré maps of Fig. 2(c) for fixed frequency excitation.

Next we use a realistic dipole moment for the molecule NO. Recent experiments have demonstrated that this molecule can be prepared in a specific vibrational excited state [26–28], and thus is a prime candidate for testing our theory. The dipole moment function is given by [24,23]

$$\mu(x) = \kappa y e^{-y/b}, \quad y = (\alpha'/\alpha)x + a, \quad (10)$$

where  $\alpha' = 1.29 \text{ \AA}^{-1}$ ,  $a = 0.1058$ ,  $b = 0.6017$ , and  $\kappa$  is chosen to satisfy  $d\mu(0)/dx = 1$ . In Fig. 3(a), we show the actions of dissociating trajectories along with the time development of their corresponding centers  $i_B(t)$ . As before, the trajectories oscillate about their centers until they reach a highly excited state, showing that they are trapped by buckets. In Fig. 3(b), we plot the Poincaré maps in the moving frame for the dissociating trajectories, and compare with the Poincaré maps for fixed frequency excitation shown in Fig. 3(c). Again, the phase portraits resemble those of  $K(\psi, J)$ . It is interesting to note that the Poincaré map of the trajectory with initial conditions  $i(0) = 0.43719$ ,  $\theta(0) = 0$  contains islands which also appear in the fixed frequency excitation case. Thus, the idea of trajectories trapped by the bucket appears to be applicable even though the approximate Hamiltonian of Eq. (6), which cannot give islands in the phase portrait, has become less accurate.

We can observe from Figs. 2(a) and 3(a) that once the systems have been carried up convectively to highly excited states, they begin to depart from the centers  $i_B(t)$ . In such excited states, the laser field is strong enough to bring the system into the chaotic regime. Then our resonance model breaks down, but the system continues to diffuse to dissociation. This scenario can be illustrated by comparing the lifetime distribution of the trajectories in phase space for chirped excitation with that for fixed frequency excitation. We observe that the nondissociating resonance zone during fixed frequency excitation becomes dissociative when acted upon by a chirped pulse, as expected from bucket dynamics consideration. In the highly excited areas (with  $i$  close to 1), however, the two distributions are quite similar, indicating that chaotic diffusion is responsible for dissociation.

Hence, the idea of bucket dynamics applies equally well to the cases of nonlinear chirping and to molecules with realistic dipole moment functions, even though it was based on the approximate Hamiltonian of Eq. (6) derived for linear chirping and a linear dipole moment.

### III. QUANTUM-MECHANICAL STUDIES

To find out how the classical predictions compare to the quantum ones, we have carried out quantum-mechanical calculations for the molecule NO using the Feit-Fleck Fourier-grid (or split-operator) method [29]. Assuming that the NO molecule is initially in a given vibrational eigenstate  $\phi_{n_0}(x)$  of the Morse oscillator of Eq. (1), we propagate the wave

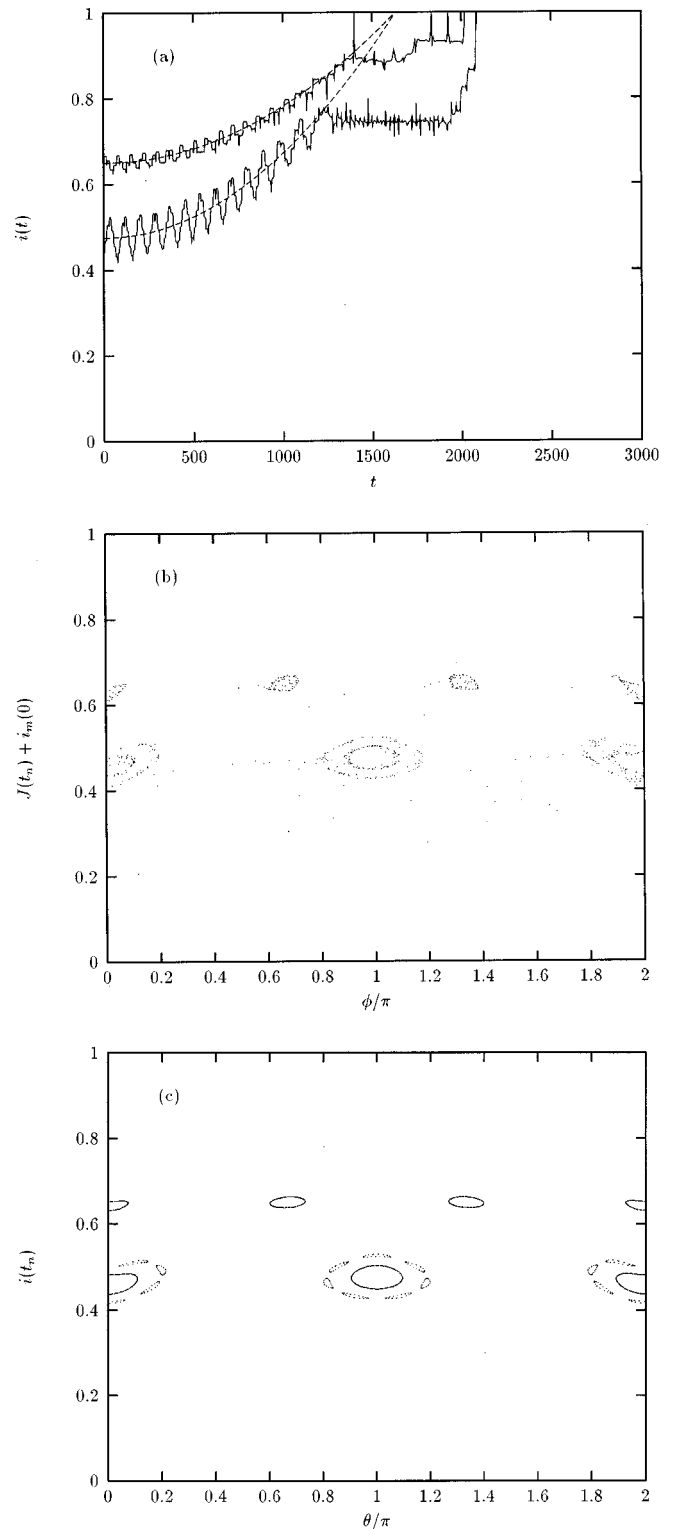


FIG. 3. Excitation using a realistic dipole moment function of NO, Eq. (10). (a) Exact trajectories for a chirped laser pulse with parameters set at  $\tau_{sw} = 2000$ ,  $\Omega_0 = 1.05$ , and  $n_p = 2$ . The initial conditions for the lower trajectory are  $(i(0), \theta(0)) = (0.43719, 1.10\pi)$  with  $B = 0.01$ , while those for the upper trajectory are  $(i(0), \theta(0)) = (0.65132, 0.072\pi)$  with  $B = 0.0065$ . The dashed lines denote the trajectories of the centers of the buckets  $i_B(t)$  given by Eq. (9) for  $m = 2$  and 3. (b) Poincaré surface of section for a chirped laser pulse with parameters given in (a); (c) the Poincaré surface of section for a fixed-frequency pulse with parameters and initial conditions given in (a) except that  $n_p = 0$ .

packet  $\psi(x,t)$  using a time-evolution operator whose Hamiltonian is given by Eq. (3). The time-evolution operator is computed as a product of a series of small time-step evolution operators, which is further approximated by a split form. In this split form a potential step is propagated in between two half-step kinetic steps given by

$$e^{-iH\Delta t/\hbar} = e^{-iK\Delta t/2\hbar} e^{-iU(x,t)\Delta t/\hbar} e^{-iK\Delta t/2\hbar} + O((\Delta t)^3), \quad (11)$$

where  $K$  is the kinetic operator and  $U(x,t)$  is the potential operator, which contains both the Morse potential and the field interaction term. Due to the symmetric splitting of the kinetic step, the error involved in the factorization approximation is then of the order of  $(\Delta t)^3$  for each step. In practice, the kinetic step is evaluated in the momentum space and the potential step evaluated in the coordinate space, respectively. The transformations between the coordinate and momentum spaces are carried out using the fast Fourier transform routines. Now a wave packet on its way to dissociation will spread out and go beyond the grid boundary. Thus it is necessary to introduce an absorbing boundary condition [30] at a reasonably large interatomic distance so that the wave packet diminishes to zero smoothly at the grid boundary. This is achieved by introducing a filter function of the form  $f(x) = 1/[1 + \exp\beta(x-x_c)]$ , where  $x_c$  is well inside the grid boundary and is large enough that the bound Morse eigenfunctions have negligible values at  $x_c$ . The parameter  $\beta$  is a large number so that  $f(x)$  is essentially zero at the grid boundary. The dissociation probability as a function of time,  $P(t)$ , can then be computed as the total amount of probability removed from the initial wave packet at time  $t$  by the absorbing boundary. Alternatively, we can project out from the wave packet the component of each Morse eigenstate and calculate the dissociation probability [31] according to

$$P(t) = 1 - \sum_n |\langle \psi(x,t) | \phi_n(x) \rangle|^2, \quad (12)$$

where  $\phi_n(x)$  denotes the Morse eigenstate. These two definitions of  $P(t)$  differ only in the fact that the second definition excludes the projection of the truncated wave packet onto the continuous part of the spectrum. As time evolves, these two definitions should yield values close to each other, for the continuum part of the truncated wave packet eventually escapes to infinity, as evidenced in Fig. 4. The first definition is more reasonable and the second forms its upper bound, which assumes the same shape, but with grassy noise on top of a smooth curve. Dissociation probabilities are the quantities that we can compare directly with experiments, when it becomes available. In most of the comparison in Sec. IV, the differences between the end-of-pulse results of these two quantum definitions are small, and the first definition of  $P(t)$  employing the absorbing boundary is used in the plots. We should mention that the sharp rise of  $P(t)$  as seen in Fig. 4(a) occurs only for the realistic dipole case, but not the linear dipole case. The realistic dipole decays exponentially with the interatomic separation and allows the chirped laser to achieve only a high level of excitation at  $t=2000$  with relatively low dissociation; the system can diffuse to dissociation subsequently. Furthermore, at these field strengths,

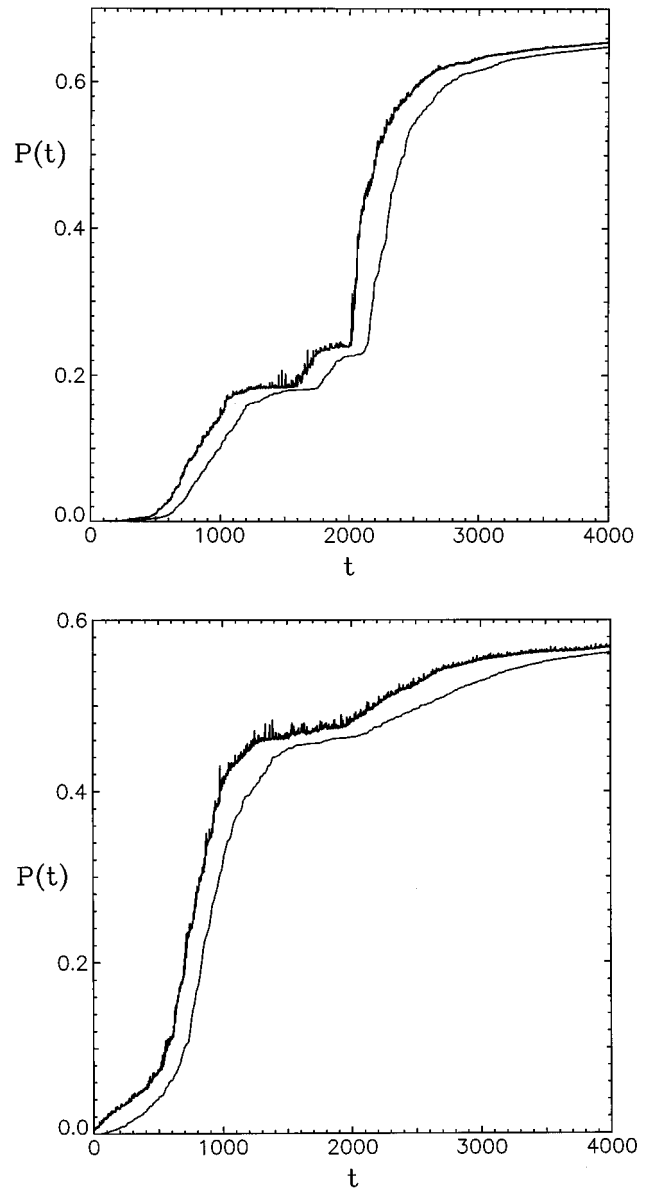


FIG. 4. Comparison between two quantum definitions of dissociation. The lighter curve denotes results using the absorbing boundary condition (see text), and the thicker line denotes results given by Eq. (12). The realistic dipole moment function is used. Time evolution of the dissociation probability is plotted for (a)  $n_0=6$ ,  $\Omega=0.9$ ,  $B=0.05$ ,  $n_p=1$ ,  $\tau_{sw}=2000$  and (b)  $n_0=40$ ,  $\Omega=1.05$ ,  $B=0.0065$ ,  $n_p=2$ ,  $\tau_{sw}=2000$ .

use of fixed frequency excitation at the outset will not produce any significant dissociation. Hence chirping is essential.

In a quantum calculation, the time evolution of the level populations during a pulse excitation can also be obtained. We assume that the molecules are in a given initial vibrational eigenstate,  $n_0$ . When the pulse arrives, some of the molecules are excited and some are de-excited by the laser field. This is best described by the time evolution of the level population distribution,  $P(n)$ , obtainable from our quantum simulation by calculating the overlaps of the wave packet with the (field-free) Morse eigenstates. We present such an example of population dynamics of NO (with realistic dipole moment) for  $n_0=6$ ,  $B=0.05$ , and  $\Omega=0.9$  in Fig. 5. At  $t=0$ ,

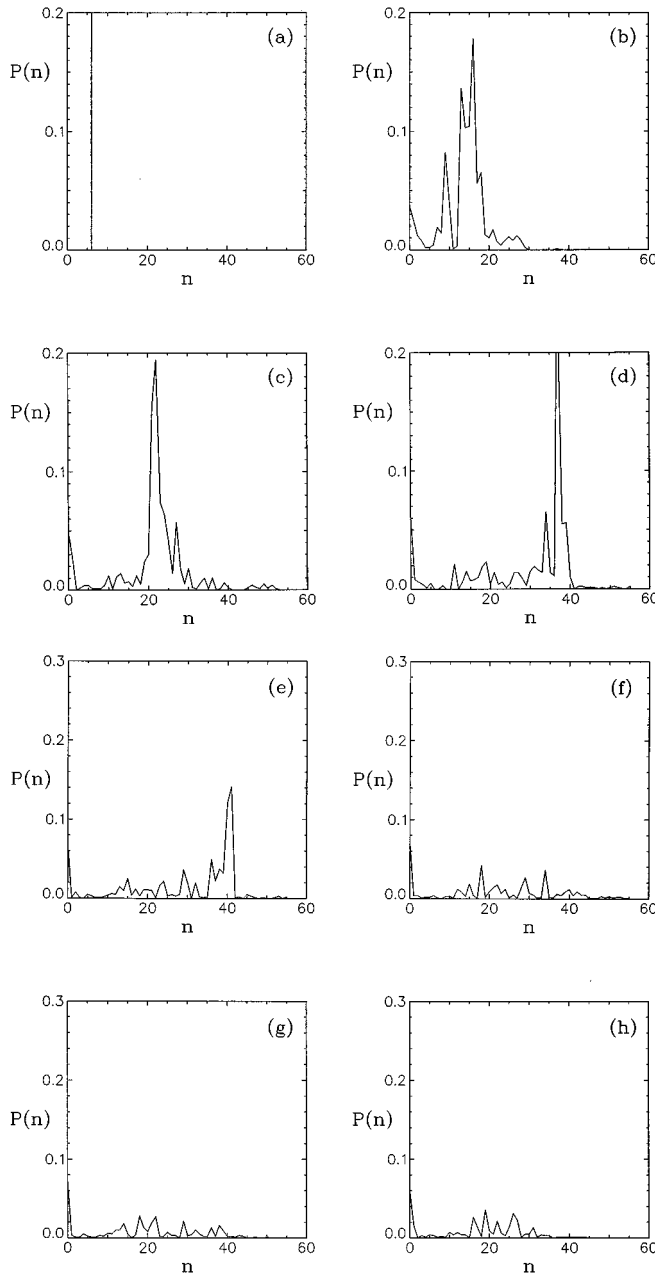


FIG. 5. Time evolution of vibrational level population of NO. The population of each vibrational quantum level is plotted against the quantum number and points are connected by straight lines to guide the eyes. Initially, only the  $n_0=6$  level is populated as shown in (a); (b) level population at 20 optical periods [ $T=2\pi/\Omega(T)$ ]; (c) at 60 T; (d) at 100 T; (e) at 140 T; (f) at 180 T, (g) at 220 T, and (h) at 260 T. The laser period becomes longer as time evolves due to chirping.

we have  $P(6)=1$  and  $P(n)=0$  for any other states  $n$ . At  $t=300.3$ , as shown in Fig. 5(b), the population has already spread out wide with the highest maximum located at  $n=16$ . The distribution reaches as high as  $n=30$  and even the  $n=37$  level has a tiny, but visible, population. There is also an appreciable peak at the ground state. As the laser pulse evolves, the highest maximum of the distribution moves to higher and higher vibrational quantum numbers. For example, the highest maximum occurs at  $n=21$  at  $t=607.8$  in

Fig. 5(c), moving to  $n=37$  at  $t=931.2$  in Fig. 5(d), and to  $n=41$  at  $t=1285.3$  in Fig. 5(e). At later times, when dissociation becomes appreciable this maximum shrinks, leaving a noisy background and a persistent peak at the ground state. This maximum may correspond to the ‘‘bucket’’ in our classical dynamics analysis.

#### IV. CLASSICAL-QUANTUM COMPARISON

In this section, we discuss the comparison between the classical and quantum results so that we can gain better understanding of the classical-quantum correspondence in driven systems [32], which may assist us in designing pathways to control chemical processes using chirped laser pulses [20,33]. The quantum dissociation probability  $P(t)$  is computed as discussed in Sec. III. To calculate  $P(t)$  classically, 1000 trajectories [34] are generated with initial angles  $\theta$  uniformly distributed between 0 and  $2\pi$ , and the initial action given by the Einstein-Brillouin-Keller (EBK) quantization condition [35]

$$i_{n_0} = (n_0 + \frac{1}{2})\hbar_{\text{eff}}, \quad n_0 = 0, 1, 2, \dots, \quad (13)$$

where the effective Planck’s constant is given in terms of the Morse parameters by

$$\hbar_{\text{eff}} = \hbar \alpha / \sqrt{2MD}. \quad (14)$$

For the NO molecule,  $\hbar_{\text{eff}}=0.017844$  [36]. After transforming the initial action-angle coordinates into Cartesian coordinates using Eq. (2), the Hamilton’s equations corresponding to the Hamiltonian of Eq. (3) are integrated numerically.  $P(t)$  is then given by the fraction of trajectories which by time  $t$  have already attained energies greater than 0 and interatomic separations greater than 10. In our numerical studies, frequency chirping is terminated at  $t=\tau_{\text{sw}}$  when  $\Omega(t)=\frac{1}{2}\Omega_0$ , and the laser frequency is kept constant at this value for the remainder of the pulse.

We first consider the dependence of the final dissociation probability,  $P_d$ , as a function of initial quantum number,  $n_0$ . In Fig. 6, we present the comparison between the classical and quantum  $P_d$  as a function of  $n_0$  ( $n$  in Fig. 6) for the diatomic molecule NO. These figures show an overall agreement between the classical and quantum results, but careful examination reveals some subtleties about the classical-quantum correspondence of driven systems. Focusing first on Fig. 6(a), where the transition dipole moment of NO is approximated by a linear function [37], we can divide the figure into two regions, separated by the initial quantum number  $n_0=38$ . In the small  $n_0$  region, there are two pronounced peaks appearing in both the classical and quantum calculations, and they correspond to the two lowest primary resonances of the Chirikov Hamiltonian given by  $i_{n_0} = 1 - (\Omega_0/m)$ ,  $m=1,2$ . Thus these resonances clearly influence both classical and quantum dynamics. The classical results in this range reveal two additional smaller resonances, which may arise from secondary resonances produced through the interactions between primary resonances. However, these two minor peaks are absent in the quantum results, which exhibit instead a single broad peak.

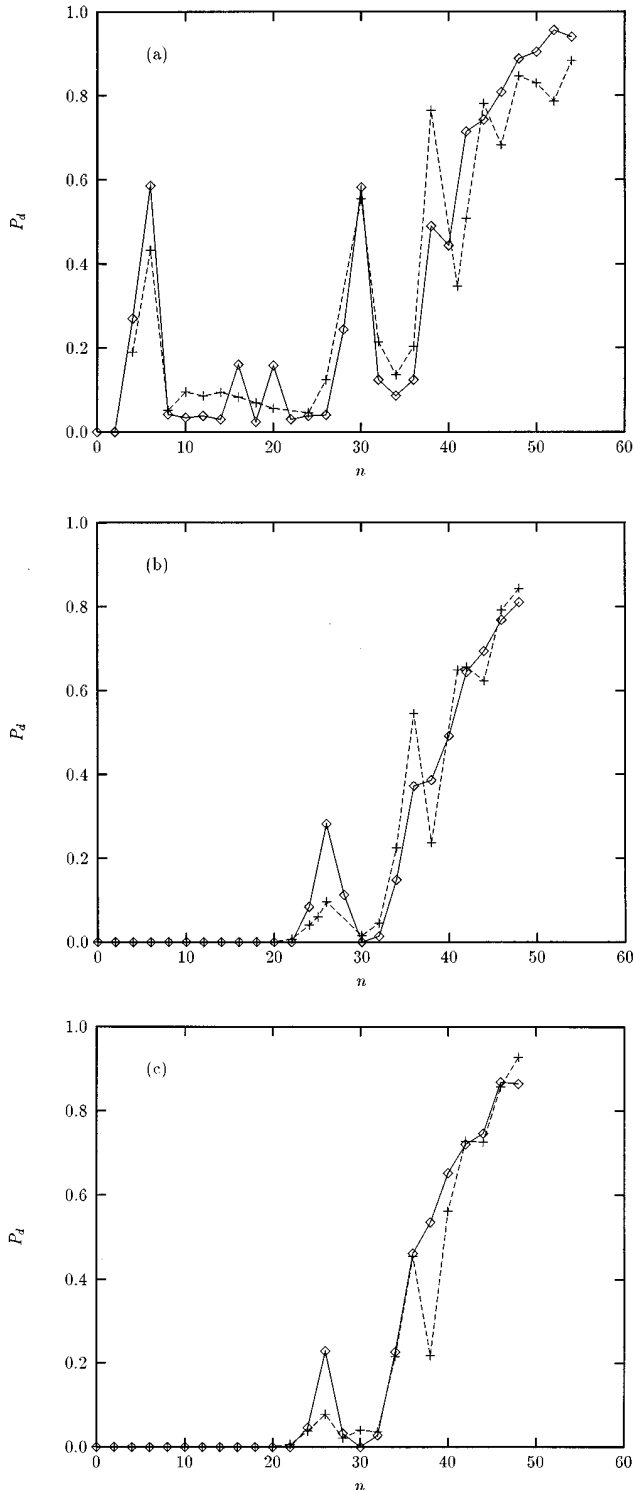


FIG. 6. Comparison between the quantum and classical dissociation probability of NO, as a function of the initial vibrational quantum number, at the end of a chirped laser pulse. The laser parameters are set at  $\tau_{sw}=2000$ , and the pulse duration is  $T_{max}=4000$ , which corresponds to 11.2 ps for NO. Chirping is turned off at  $t=\tau_{sw}$  and the laser frequency is kept fixed at  $\Omega_0/2$  until the end of the pulse. Diamonds connected by solid lines denote classical results and crosses connected by dashed lines denote quantum results. (a) Approximate linear dipole moment used at  $B=0.003$ ,  $\Omega_0=0.9$ ,  $n_p=1$ . (b) Realistic dipole moment function used at  $B=0.0065$ ,  $\Omega_0=1.05$ ,  $n_p=1$ . (c) Realistic dipole moment function used at  $B=0.0065$ ,  $\Omega_0=1.05$ ,  $n_p=2$ .

In the large  $n_0$  region of Fig. 6(a), where  $n_0 > 38$ , we see that the quantum curve still fluctuates with peaks located at higher-order primary resonances on top of a background which increases with  $n_0$ . However, the classical curve is much smoother with smaller peaks of resonance. In this energy range the phase space is chaotic; it seems that the nonlinear resonances influence quantum dynamics more pronouncedly than classical dynamics. Furthermore, in the soft-chaos region for which  $n_0$  is between 38 and 46, the quantum results oscillate around the classical curve in such a way that the classical curve resembles a smoothed version of the quantum results, but above  $n_0=46$ , the quantum curve clearly falls below the classical one.

To interpret these observations in the classical-quantum comparison, we present the following two propositions: In the soft-chaos case, cantori (remnants of resonant tori that have broken up) existing in the phase space tend to slow down the quantum flow more than the classical flow. In other words, cantori can still trap quantum flow and carry it in buckets to dissociation, while, in comparison, classical flow tends to leak through so that dissociation takes place in this energy regime mainly through the ordinary diffusive process. In the hard-chaos regime ( $n_0 > 46$ ), the fact that the quantum value falls below the classical curve could be an indication of weak quantum localization [38,39], but more work needs to be done to confirm it.

The above discussions of the multiphoton dissociation properties of NO using an approximate linear dipole moment apply equally well to the results using a more realistic dipole moment function, as shown in Figs. 6(b) and 6(c). However, the features of these plots are not as clearly manifest as in Fig. 6(a). Furthermore, the effects of varying the order of chirping,  $n_p$ , can be observed by comparing the two quantum curves of Figs. 6(b) and 6(c): at this sweeping rate ( $\tau_{sw}=2000$ ), quadratic chirping is slightly more effective than linear chirping in promoting dissociation.

We can examine the correspondence between classical and quantum dynamics even more closely by following the time evolution of dissociation probabilities,  $P(t)$ , as shown in Fig. 7. In all cases shown, there is strong similarity in the shapes of the curves, such as the sudden rise of  $P(t)$  at about the same time, and multiple thresholds of the curves. This multithreshold behavior appears to be a common feature of  $P(t)$ , when the realistic dipole moment of Eq. (10) is used (see also Fig. 4). The second threshold occurs at time  $t \sim \tau_{sw}=2000$  when chirping is switched off and the laser pulse assumes a constant frequency at  $1/2\Omega_0$ . To interpret this phenomenon classically, we refer to Fig. 3(a), which is under a similar situation. The system is excited to a high value of  $i$  at  $t=\tau_{sw}=2000$  by the chirped pulse. After chirping is switched off, the system under the action of fixed frequency excitation at  $1/2\Omega_0$  is chaotic. It immediately diffuses to dissociation as shown in the figure, resulting in the sudden rise in  $P(t)$ . Detailed studies of the classical dissociation dynamics under various pulse shape and chirping conditions will be presented in a forthcoming paper [40].

The strong similarity between the classical and the quantum results is encouraging, for it implies that in most cases the phase space structures influence both the classical and quantum dynamics alike. Therefore, nonlinear dynamics can be used to provide us with useful physical pictures, and thus

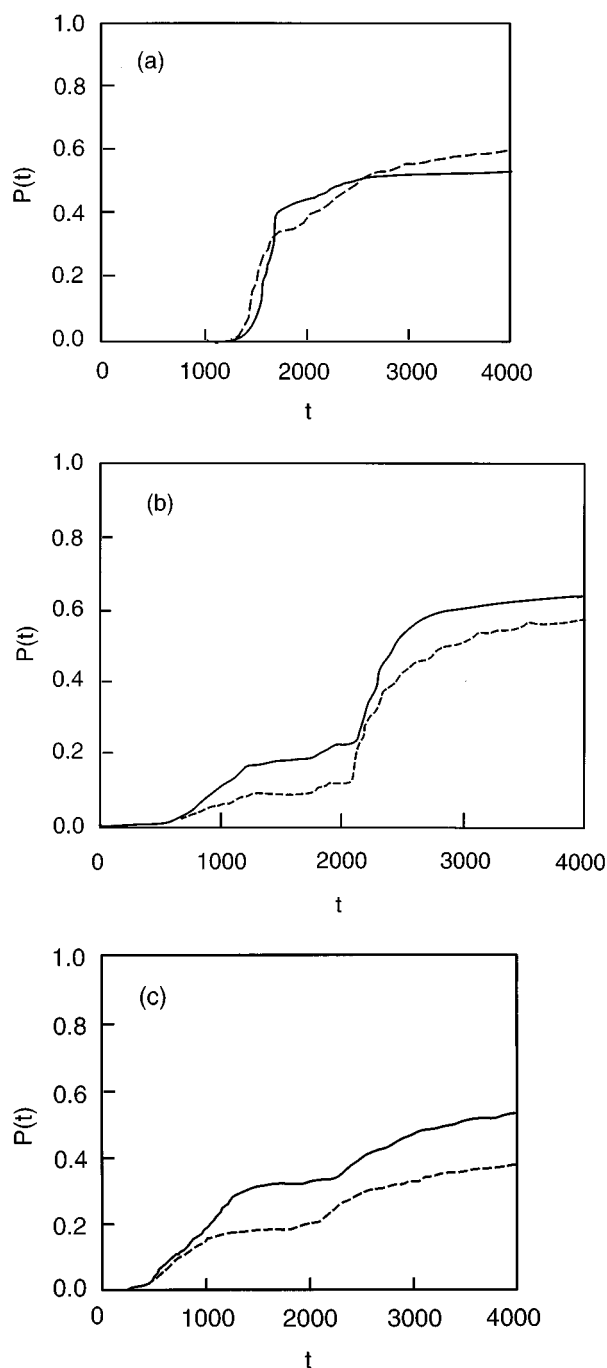


FIG. 7. Time evolution of the dissociation probability during a chirped laser pulse where  $\tau_{\text{sw}}=2000$  and  $T_{\text{max}}=4000$ . Solid lines denote quantum results and dashed lines denote classical results. (a) Parameters are  $n_0=30$ ,  $B=0.003$ ,  $\Omega_0=0.9$ ,  $n_p=2$  and linear dipole function used. (b)  $n_0=6$ ,  $B=0.05$ ,  $\Omega_0=0.9$ ,  $n_p=2$  and realistic dipole function used. (c)  $n_0=36$ ,  $B=0.0065$ ,  $\Omega_0=1.05$ ,  $n_p=1$  and realistic dipole function used.

deeper understanding, of the chirped processes involved. More importantly, we can make use of the classical phase space dynamics to design pathways to control chemical processes when a chirped laser pulse is employed and quantum coherence does not play a key role.

## V. DISCUSSION

In the present paper we study the effects upon the dissociation dynamics achieved by varying the initial vibrational states, the sweeping rate, the order of frequency chirping, field strength and frequency, and the functional form of the dipole moment function. Our results show that in all cases investigated the bucket dynamic model is very useful in predicting the dynamical behavior of the chirped processes. Therefore, it provides an analytical base for the frequency control of a laser pulse to climb an anharmonic ladder.

We should point out that when the linear approximation to the dipole moment function is valid, the classical results are universal in the sense that there is only one scaled curve for each excitation property for all diatomic molecules. The quantum results, however, vary from molecule to molecule, depending primarily on the total number of bound states,  $N_b$ , that a Morse oscillator can support. Since the action for bound state motion must satisfy  $i \leq 1$ , we obtained from the EBK quantization condition of Eq. (13) that  $N_b = \text{int}(1/\hbar_{\text{eff}} + 1/2)$ . Thus an effective Planck constant [5] arises in the Morse oscillator systems that is inversely proportional to  $N_b$ . According to Bohr's correspondence principle, we expect the classical-quantum correspondence to improve as the effective Planck constant decreases or as the number of bound states increases. To verify this numerically, we should study several diatomic molecules with different  $N_b$ . This is one of the main reasons that we chose to study NO, which has 56 bound Morse states. Much of our earlier work has focused on HF [5], a popular system used in the study of infrared multiphoton dissociation with 24 bound states. However, a systematic comparison between these two systems has yet to be made.

Another reason to study NO is that, as suggested to us by Bergmann, it is a molecule that can be prepared in some highly excited vibrational states by stimulated Raman adiabatic passage [27], or by the stimulated emission pumping technique of Wodtke and co-workers [26]. Finally, the idea of "dynamic autoresonance" introduced in the multiphoton ionization of Rydberg atoms and kicked rotors [41] is very similar to that of bucket dynamics, except the former invokes further approximations to the Chirikov Hamiltonian. Both are useful for the analysis of chirped processes.

## ACKNOWLEDGMENTS

We are grateful to Professor Peter Koch, Professor Klass Bergmann, Professor Paul Corkum, Professor Andre D. Bandauk, Professor S. Chelkowski, and Professor Donna Strickland for stimulating discussions. Part of this work was performed when W.K.L. was visiting the Institute of Atomic and Molecular Sciences, Academia Sinica, Taiwan; we thank Professor S.H. Lin for his continuing interest in our work, and the NSC of the Republic of China for its support. This work was partially supported by a Natural Sciences and Engineering Research Council (NSERC) of Canada Research grant to W.K.L., and by the National Science Foundation through Grant No. PHY-9408879 to J.M.Y.

## APPENDIX

In this appendix, we provide a detailed derivation of the resonant Hamiltonian, Eq. (6), for the case of a linear dipole moment function  $\mu(x)=x$ . Substituting Eq. (2) into the Hamiltonian of Eq. (3), and using the Fourier expansion of  $x(\cos \theta)$  [25,11,13], the Hamiltonian can be expressed in action-angle variables as

$$H(\theta, i, t) = H_0(i) - B \left\{ G_0 \cos \Omega t - \sum_{n=1}^{\infty} G_n [\cos(n\theta - \Omega t) + \cos(n\theta + \Omega t)] \right\}, \quad (\text{A1})$$

where  $H_0(i) = -\frac{1}{2}(1-i)^2$ ,  $G_0 = \ln[(1-i/2)/(1-i)^2]$ , and  $G_n = 1/n [i/(2-i)]^{n/2}$ . Expanding  $H$  about the resonant action  $i_m$  of Eq. (5) to second order in  $j = i - i_m$  and keeping only the resonant term  $G_m \cos(m\theta - \Omega t)$  (the rotating wave approximation), we obtain the Chirikov Hamiltonian

$$H_r(\theta, j, t) = -\frac{j^2}{2} + \frac{\Omega}{m} j + B G_m \cos(m\theta - \Omega t), \quad (\text{A2})$$

where, consistent with the assumption of adiabatic invariance, we have ignored the time dependence of  $i_m$ , and the constant term  $H_0(i_m)$  has been omitted in Eq. (A2). Following Ref. [21], a transformation to the moving frame with

$$\phi = \theta - \frac{\Omega}{m} t, \quad I = j + \frac{\dot{\Omega}}{m} t, \quad (\text{A3})$$

can be achieved by the generating function

$$F_2(\theta, I, t) = \left( \theta - \frac{\Omega}{m} t \right) I - \theta \frac{\dot{\Omega}}{m} t + h(t), \quad (\text{A4})$$

satisfying  $\phi = \partial F_2(\theta, I, t) / \partial I$  and  $I = \partial F_2(\theta, I, t) / \partial \theta$ . If  $h(t)$  in Eq. (A4) is chosen to satisfy

$$\frac{dh}{dt} = \frac{1}{m^2} \left( \dot{\Omega} \Omega t + \Omega t \frac{d}{dt} (\dot{\Omega} t) + \frac{1}{2} (\dot{\Omega} t)^2 \right),$$

the new Hamiltonian in  $(\phi, I)$  takes the simple form

$$H'_r(\phi, I) = H_r + \frac{\partial F_2}{\partial t} = -\frac{I^2}{2} + B G_m \cos m\phi - \frac{\phi}{m} \frac{d}{dt} (\dot{\Omega} t). \quad (\text{A5})$$

Making a further canonical transformation to  $J=I$  and  $\psi = -\phi$  and noting that the Jacobian of this transformation equals  $-1$ , the final Hamiltonian in terms of  $(J, \psi)$  is given by

$$K(\psi, J) = -H'_r(-\psi, J),$$

which yields Eq. (6).

- 
- [1] N. R. Isenor and M. C. Richardson, *Appl. Phys. Lett.* **18**, 224 (1971).
- [2] R. V. Ambartsumian, V. S. Letokhov, E. A. Ryabov, and N. V. Chekalin, *Pis'ma Zh. Eksp. Teor. Fiz.* **20**, 597 (1974) [*JETP Lett.* **20**, 273 (1974)].
- [3] D. S. King, in *Dynamics of the Excited State*, edited by K. P. Lawley (Wiley, New York, 1982), pp. 105–189; S. K. Gray, J. R. Stine, and D. W. Noid, *Laser Chem.* **5**, 209 (1985).
- [4] N. Bloembergen, C. D. Cantrell, and D. M. Larsen, in *Tunable Lasers and Applications*, edited by A. Mooradian and P. Stokseth (Springer, New York, 1976); M. J. Coggiola, P. A. Schulz, Y. T. Lee, and Y. R. Shen, *Phys. Rev. Lett.* **38**, 17 (1977).
- [5] R. B. Walker and R. K. Preston, *J. Chem. Phys.* **67**, 2017 (1977).
- [6] J. F. Heagy, Z. M. Lu, J. M. Yuan, and M. Vallières, in *Directions in Chaos*, edited by D. H. Feng and J. M. Yuan (World Scientific, Singapore, 1992), pp. 322–396, and references cited therein.
- [7] R. Wallace, *Chem. Phys.* **11**, 189 (1975); B. R. Henry, *Acc. Chem. Res.* **10**, 207 (1977).
- [8] M. C. Gutzwiller, *Chaos in Classical and Quantum Mechanics* (Springer-Verlag, New York, 1990).
- [9] Quantum and Chaos: How Incompatible?, special issue of *Prog. Theor. Phys. Suppl.* **116** (1994).
- [10] G. M. Zaslavskii and B. V. Chirikov, *Usp. Fiz. Nauk.* **105**, 3 (1971) [*Sov. Phys. Usp.* **14**, 549 (1972)]; A. J. Lichtenberg and M. A. Lieberman, *Regular and Stochastic Motion* (Springer, New York, 1980), Sect. 5.6; R. V. Jensen, *Phys. Rev. A* **30**, 386 (1984).
- [11] Y. Gu and J. M. Yuan, *Phys. Rev. A* **36**, 3788 (1987).
- [12] J. Heagy and J. M. Yuan, *Phys. Rev. A* **41**, 571 (1990).
- [13] B. Wu and W.-K. Liu, *Phys. Rev. A* **205**, 470 (1994).
- [14] B. V. Chirikov, *Phys. Rep.* **52**, 263 (1979).
- [15] S. Chelkowski, A. D. Bandrauk, and P. B. Corkum, *Phys. Rev. Lett.* **65**, 2355 (1990).
- [16] S. Chelkowski and A. D. Bandrauk, *Chem. Phys. Lett.* **186**, 264 (1991); in *Coherence Phenomena in Atoms and Molecules in Laser Fields*, Vol. 287 of *NATO Advanced Study Institute Series B: Physics*, edited by A. D. Bandrauk (Plenum, New York, 1992), p. 333.
- [17] S. Chelkowski and A. D. Bandrauk, *J. Chem. Phys.* **99**, 4279 (1993); S. Chelkowski and G. N. Gibson, *Phys. Rev. A* **52**, R3417 (1995).
- [18] P. Dietrich and P. B. Corkum, *J. Chem. Phys.* **97**, 3187 (1992).
- [19] S. Krempf, T. Eisenhammer, A. Hüber, G. Mayer-Kress, and P. W. Milonni, *Phys. Rev. Lett.* **69**, 430 (1992).
- [20] J. S. Melinger, D. McMorrow, C. Hillegas, and W. S. Warren, *Phys. Rev. A* **51**, 3366 (1995).
- [21] C. T. Hsu, C. Z. Cheng, P. Helander, D. J. Sigmar, and R. White, *Phys. Rev. Lett.* **72**, 2503 (1994).
- [22] T. C. Marshall, *Free-Electron Lasers* (MacMillan, New York, 1985), p. 55.
- [23] W.-K. Liu, B. Wu, and J. M. Yuan, *Phys. Rev. Lett.* **75**, 1292 (1995).
- [24] T. F. Jiang (private communications); F. P. Billingsley II, *J. Chem. Phys.* **62**, 864 (1975).

- [25] D. Richards, *Introduction to Non-linear Dynamics*, Open University Third Level Course MS 323 (The Open University, Milton Keynes, New York, 1990), Unit 10; P. A. Dando and D. Richards, *J. Phys. B* **23**, 3179 (1990).
- [26] X. Yang and A. M. Wodtke, *J. Chem. Phys.* **92**, 116 (1990); X. Yang, E. H. Kim, and A. M. Wodtke, *ibid.* **96**, 5111 (1992).
- [27] S. Schiemann, A. Kuhn, S. Steuerwald, and K. Bergmann, *Phys. Rev. Lett.* **71**, 3637 (1993).
- [28] D. J. Mass, D. I. Duncan, A. F. G. van der Meer, W. J. van der Zande, and L. Noordam (unpublished).
- [29] M. D. Feit, J. A. Fleck, and A. Steiger, *J. Comput. Phys.* **47**, 412 (1982); R. Kosloff, *Annu. Rev. Phys. Chem.* **45**, 145 (1994); D. Kosloff and R. Kosloff, *J. Comput. Phys.* **52**, 35 (1983); C. Leforestier *et al.*, *ibid.* **94**, 59 (1991).
- [30] R. Heather and H. Metiu, *J. Chem. Phys.* **86**, 5009 (1987); **88**, 5496 (1988).
- [31] M. E. Gogggin and P. W. Milonni, *Phys. Rev. A* **37**, 796 (1988).
- [32] J. M. Yuan, Z. M. Lu, M. Vallieres, and J. F. Heagy, *Prog. Theor. Phys. Suppl.* **116**, 425 (1994).
- [33] P. Brumer and M. Shapiro, *Acc. Chem. Res.* **22**, 407 (1993); W. S. Warren, H. Babitz, and M. Dahleh, *Science* **259**, 1581 (1993).
- [34] In typical testing cases, comparison between runs using 500 and 1000 trajectories shows that the results converge to within a few percent, the worse case being 5.4%.
- [35] I. C. Percival, *Adv. Chem. Phys.* **36**, 1 (1977).
- [36] K. P. Huber and G. Herzberg, *Molecular Spectra and Molecular Structure: IV. Constants of Diatomic Molecules* (van Nostrand Reinhold, New York, 1979).
- [37] A linear approximation to a dipole moment function may be appropriate for the study of molecular excitation, but it has the wrong asymptotic limit for dissociation into neutral products. On the other hand, if one is mainly interested in the effects of varying the depth of a Morse potential on dissociation, linear dipole moment functions can be assumed for all molecules investigated.
- [38] D. R. Grepel, R. E. Prange, and S. Fishman, *Phys. Rev. A* **29**, 1639 (1984); S. Fishman, D. R. Grepel, and R. E. Prange, *Phys. Rev. Lett.* **49**, 509 (1982).
- [39] R. A. Jalabert, H. U. Baranger, and A. D. Stone, *Phys. Rev. Lett.* **65**, 2442 (1990).
- [40] W.-K. Liu, J. M. Yuan, and S. Lin (unpublished).
- [41] B. Meerson and S. Yariv, *Phys. Rev. A* **44**, 3570 (1991); B. Meerson and L. Friedland, *ibid.* **41**, 5233 (1990).